AIAA JOURNAL
Vol. 32, No. 12, December 1994

Identification of Impact Forces at Multiple Locations on Laminated Plates

Enboa Wu* and Jung-Cheng Yeh†
National Taiwan University, Taipei, Taiwan 106, Republic of China
and
Ching-Shih Yen‡
Fushin Institute of Technology, Toucheng, Ilan, Taiwan 261, Republic of China

This paper presents an analytical method for the identification of force histories on a rectangular laminated plate when it is struck by foreign objects at multiple locations. The governing equations of motion of the plate are constructed by using the classical lamination theory and the Rayleigh-Ritz method. The modal superposition method is then employed to obtain Green's function in a transformed time domain. To obtain the impact force histories exerted at multiple locations on the laminate, a constrained optimization method has been employed. The method has been verified using both randomly generated numerical signals with a signal-to-noise ratio of 1.0 and experimental data. The agreement is satisfactory in all of the comparisons. The method is then applied to further identify the actual impact points among several locations on a laminate that may be hit. With minor modifications, this method is also applied to reconstruct the strain histories, a portion of which are accidently lost in an impact event.

Introduction

BECAUSE of the tendency for invisible damage to occur inside structures made of advanced composite materials, study of the low-velocity-impact response of composite laminates has attracted the attention of many researchers during recent decades. Most of the work has involved analyzing the responses of a laminated structure when the initial configurations of the structure and the impactor are known.[1] To obtain the relationship between the impactor movement and the plate motion at the impact location, the force-indentation relationship has been frequently applied. This relationship may be obtained by experiment,[1,2] by Hertz contact law,[3] or by more rigorously theoretical derivations.[4,5] In addition, the laminates analyzed may be subjected to in-plane prestressed loading,[6] large deflection,[7] or various types of damage.[8] On the other hand, experimental results have been reported for the investigation of the responses of laminated structures subjected to single[1,2,8] or repeated[2,9] impact loading at low striking velocities. The relationship between a laminated plate subjected to low-velocity impact and to quasistatic contact was also reported.[2,10] When the initial striking velocity of the projectile was higher, the focus was on investigation of the ballistic resistance capability of the composite materials.[11,12]

An alternate approach to understanding the impact behavior of a composite structure is to use the inverse method. When the impact duration is short such that wave motion dominates the impact response, the generalized ray theory is frequently employed.[13,14] As the impact duration becomes longer, such as in low-velocity impact by a foreign object, the generalized ray theory becomes not applicable because stress waves are reflected many times from the boundaries of a structure. To overcome this problem, Doyle has proposed a frequency domain method using a complicated filtering procedure to suppress the effect of this wave reflection and has successfully identified the impact force of a duration longer than 1 ms.[15,16]

Another method for identifying the impact force history with a duration on the order of 1 ms is to use the modal superposition method. Hollandsworth and Busby[17] have identified the impact force exerted on a cantilever beam using the response recorded by an accelerometer as the input data. For a circular plate struck at its center, Wu et al.[18] have constructed Green's functions from a series of Bessel functions. An optimization method was employed to search for the optimal impact force history. In the same paper, they also proposed an experimental method, by which the impact force history could be identified through a simple deconvolution process. This empirical method can thus be applied to structures with complicated material properties or boundary conditions. However, responses of a structure to impact of foreign objects acting simultaneously at multiple locations have not been addressed by any of the aforementioned studies.

In this paper, an analytical method has been developed to identify the force histories of a composite laminate when it is struck by foreign objects at multiple locations. This situation may be encountered when a flying vehicle is passing through a region with rain, dust, or hail. In other situations, multiple dents may be found on the surface of a laminated structure such that it is hard to determine whether single or multiple impact occurred. For all of these situations, the method developed in this paper can be used to identify the impact force histories from the recorded strain histories. Further, this method can be extended to reconstruct the strain histories when a portion of the strains are not recorded due either to an improper triggering setting or to unexpectedly large signals occurring in an impact event. To develop this analytical method, a rectangular composite laminated plate will be modeled by using the classical lamination theory, and the Rayleigh-Ritz method will be employed to form the governing equations of motion of the plate. The modal superposition method will then be applied to construct Green's functions, which will be used to relate the forces exerted at multiple locations to the responses of the plate. Meanwhile, the gradient projection method will be applied to search for the optimal impact force histories. Both numerical data with a signal-to-noise ratio of 1.0 and experimental data will then be used to verify the proposed method.

Analytical Method

Governing Equations

The displacement field of the laminated plate shown in Fig. 1 can be expressed in the following form if the classical lamination theory is adopted:

$$\begin{aligned} u_x(x, y, z, t) &= -z\frac{\partial w}{\partial x}(x, y, t) \\ u_y(x, y, z, t) &= -z\frac{\partial w}{\partial y}(x, y, t) \\ u_z(x, y, z, t) &= w(x, y, t) \end{aligned} \tag{1}$$

Received Oct. 12, 1993; revision received March 11, 1994; accepted for publication March 17, 1994.

*Associate Professor, Institute of Applied Mechanics.
†Graduate Student, Institute of Applied Mechanics.
‡Associate Professor, Department of Mechanical Engineering.

where u_x and u_y are the displacements in the x and y directions, respectively; and w is the lateral displacement and is the only independent variable. In this study, this lateral displacement field is expressed in the following form by applying the Rayleigh-Ritz method[19–21]:

$$w(x, y, t) = \sum_{i,j} w_{ij}(t)\xi_i(x)\eta_j(y) \tag{2}$$

where $\xi_i(x)$ and $\eta_j(y)$ are the vibrating modes of Euler beams (beam functions) satisfying the boundary conditions in the x and y directions, respectively; and $w_{ij}(t)$ is the generalized coordinate associated with the kinematically admissible displacement, $\xi_i(x)\eta_j(y)$. The strain-displacement and the constitutive relationships can then be applied to calculate the strains and the stresses, respectively.

The Hamilton principle is employed to obtain the governing equations of motion of the laminated plate. The kinetic and strain energies, respectively, read

$$T = \frac{1}{2}\int_0^b \int_0^a \int_{-\frac{h}{2}}^{\frac{h}{2}} \rho\left(\dot{u}_x^2 + \dot{u}_y^2 + \dot{u}_z^2\right) dz\, dx\, dy \tag{3}$$

and

$$V = \frac{1}{2}\int_0^b \int_0^a \int_{-\frac{h}{2}}^{\frac{h}{2}} (\sigma_x\epsilon_x + \sigma_y\epsilon_y + 2\tau_{xy}\epsilon_{xy})\, dz\, dx\, dy \tag{4}$$

where ρ, a, b, and h are the density, dimensions in the x and y directions, and thickness of the laminated plate, respectively. The work done by the applied multiple impact loads is

$$W = \sum_{i=1}^{L} \int_0^b \int_0^a P^i u_z\, dx\, dy \tag{5}$$

where L is the number of the impact forces applied, and $P^i = P^i(x_i, y_i, t)$ is the ith impact force acting in the z direction of the plate. Thus, the equations of motion of the plate are

$$[M]\{\ddot{q}\} + [K]\{q\} = \sum_{i=1}^{L}\{\bar{P}^i\} \tag{6}$$

where q is the vector formed by $w_{ij}(t)$. In Eq. (6), the mass matrix $[M]$ and the stiffness matrix $[K]$ are both of order $N \times N$, where $N = N_1 \times N_2$, and N_1 and N_2 are the numbers of beam functions in the x and y directions, respectively. The value of each element of these two matrices can then be calculated directly. On the other hand, each of the exerted impact forces is assumed to be a point load. Thus, the generalized force is

$$\{\bar{P}^i\} = P^i(t)\{Y\}_{(x_i,y_i)} \tag{7}$$

where

$$\{Y\}^T = \{\xi_1\eta_1, \xi_2\eta_1, \ldots, \xi_1\eta_2, \xi_2\eta_2, \ldots\}$$

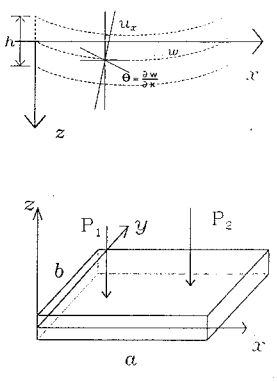

Fig. 1 Coordinate system, applied forces, and deformation of a laminated plate.

and (x_i, y_i) is the impact location corresponding to the ith impact force P_i on the plate.

Green's Functions

To obtain Green's functions, which correlate the forces exerted at multiple locations on the plate to the plate response, the modal superposition method is employed. Thus, the right-hand side of Eq. (6) is set to be zero to obtain N number of natural frequencies (eigenvalues), $\omega_1, \omega_2, \ldots, \omega_N$, and the corresponding modal shapes (eigenvectors), $\{e_1\}, \{e_2\}, \ldots, \{e_N\}$. Because the vibrating modes, each of which is constructed by the N beam functions, are orthogonal, the vector $\{q\}$ can be expressed as

$$\{q\} = \sum_{j=1}^{N} a_j(t)\{e_j\} = [X]\{a\} \tag{8}$$

where

$$[X] = [\{e_1\}, \{e_2\}, \ldots, \{e_N\}] \tag{9}$$

and

$$\{a\}^T = \{a_1, a_2, \ldots, a_N\} \tag{10}$$

is the vector formed by the generalized coordinates of the dynamic system expressed in Eq. (6). Thus, a system of decoupled ordinary differential equations can be obtained as

$$m_j\ddot{a}_j + k_j a_j = \sum_{i=1}^{L} P^i(t)\{e_j\}^T\{Y\}_{(x_i,y_i)} \qquad j = 1, \ldots, N \tag{11}$$

where

$$m_j = \{e_j\}^T[M]\{e_j\}$$

$$k_j = m_j\omega_j^2$$

Letting the plate remain stationary before impact, Eq. (11) can be integrated in terms of the following convolution integral:

$$a_j(t) = \sum_{i=1}^{L} \frac{\{e_j\}^T\{Y\}_{(x_i,y_i)}}{m_j\omega_j} \int_0^t P^i(\tau)\sin[\omega_j(t-\tau)]\, d\tau, \qquad j = 1, \ldots, N \tag{12}$$

By assuming that the impact force $P^i(\tau)$ varies linearly within a time step, Δt, Eq. (12) is expressed in the following form at $t = t_k$ as

$$a_{j(k)} = \sum_{i=1}^{L}\{e_j\}^T\{Y\}_{(x_i,y_i)}\left[\sum_{s=1}^{k-1} R(k-s, j)P_s^i + T(j)P_k^i\right] \tag{13}$$

where

$$R(l, j) = \frac{1}{k_j\omega_j\Delta t}[-\sin(\omega_j t_{l-1}) + 2\sin(\omega_j t_l) - \sin(\omega_j t_{l+1})] \tag{14}$$

$$T(j) = \frac{1}{k_j}\left[1 - \frac{\sin(\omega_j\Delta t)}{\omega_j\Delta t}\right] \tag{15}$$

For rigid-body modes, i.e., $\omega_j = 0$, the previous two equations read

$$R(l, j) = l(\Delta t)^2/m_j \tag{16}$$

$$T(j) = (\Delta t)^2/(6m_j) \tag{17}$$

Thus, at $t = t_k$, Eq. (8) becomes

$$\{q\}_k = [X]\{a\}_k \tag{18}$$

At a strain gauge location, e.g., $(x_s, y_s, h/2)$, the strain response at $t = t_k$ is

$$\epsilon_\zeta = \sum_{i=1}^{L}\sum_{j=1}^{k} G^i_{k+1-j} P^i_j \tag{19}$$

where

$$G^i_1 = -h/2 \cdot \{\Gamma_\zeta\}^T [X][T][X]^T \{Y\}_{(x_i,y_i)} \tag{20}$$

$$G^i_{j+1} = -h/2 \cdot \{\Gamma_\zeta\}^T [X][R][X]^T \{Y\}_{(x_i,y_i)} \qquad k \geq j \geq 1 \tag{21}$$

$$[R] = \text{diag}\,[R(j,1), R(j,2), \ldots] \tag{22}$$

$$[T] = \text{diag}\,[T(1), T(2), \ldots] \tag{23}$$

$$\{\Gamma_\zeta\}^T = \begin{cases} \{\xi''_1\eta_1, \xi''_2\eta_1, \ldots, \xi''_{N_1}\eta_1, \xi''_1\eta_2, \ldots, \xi''_{N_1}\eta_{N_2}\}_{(x_s,y_s)} \\ \qquad \text{if } \zeta = x \\ \{\xi_1\eta''_1, \xi_2\eta''_1, \ldots, \xi_{N_1}\eta''_1, \xi_1\eta''_2, \ldots, \xi_{N_2}\eta''_{N_1}\}_{(x_s,y_s)} \\ \qquad \text{if } \zeta = y \end{cases} \tag{24}$$

and diag is a diagonal matrix.

If one expresses Eq. (19) at $t = t_1, t_2, \ldots, t_n$, the following matrix form can be obtained:

$$\begin{Bmatrix} r_1 \\ r_2 \\ r_3 \\ \vdots \\ r_n \end{Bmatrix} = \sum_{i=1}^{L} \begin{bmatrix} G_1 & & & & \\ G_2 & G_1 & & 0 & \\ G_3 & G_2 & G_1 & & \\ \vdots & \vdots & \vdots & \ddots & \\ G_n & G_{n-1} & G_{n-2} & \cdots & G_1 \end{bmatrix}_i \begin{Bmatrix} P_1 \\ P_2 \\ P_3 \\ \vdots \\ P_n \end{Bmatrix}_i \tag{25}$$

where n is the number of the time steps used to discretize Eq. (19) in time.

Inverse Method

Equation (25) can further be expressed in a form as

$$\mathbf{r} = \sum_{i=1}^{L} \mathbf{G}_i \mathbf{P}_i \tag{26}$$

where $\boldsymbol{r}$ and $\boldsymbol{P_i}$ are $n \times 1$ vectors, and $\boldsymbol{G_i}$ is an $n \times n$ matrix. In the inverse problem, $\boldsymbol{P_i}$ are the unknowns to be obtained. Note that the response recorded by a single gauge is not sufficient to identify the impact force histories. This is because the number of unknowns is greater than the amount of recorded strain data. Therefore, multiple gauges are needed, and the following condition must hold:

$$\mathbf{r}_j = \sum_{i=1}^{L} \mathbf{G}_{ji} \mathbf{P}_i; \qquad j = 1, \ldots, M, \qquad M \geq L \tag{27}$$

where M is the number of the gauges used.

In view of the ill-posed characteristics of Green's functions, $\boldsymbol{G_{ji}}$, Eq. (27) is converted into the following error function and is solved by using the optimization technique:

$$E = \sum_{j=1}^{M} \left(\mathbf{r}_j - \sum_{i=1}^{L} \mathbf{G}_{ji}\mathbf{P}_i\right)^T \left(\mathbf{r}_j - \sum_{i=1}^{L} \mathbf{G}_{ji}\mathbf{P}_i\right), \qquad M \geq L \tag{28}$$

In this study, the gradient projection method,[22] which is a constrained optimization method, is used to solve Eq. (28). The only constraint employed in the process of searching for the impact forces is that the applied forces must always be in compression, i.e., always in the $-z$ direction (Fig. 1). Expanding Eq. (28), a quadratic form of the unknowns, $\boldsymbol{P_i}$, is obtained. Therefore, the impact forces optimally searched must be such that the error function E is of the global minimum value, which is thus the solution of interest.

Numerical Verification

Results and Discussion

Numerical verification was performed by striking a freely supported T300/976 Gr/ep $[0^\circ_4/90^\circ_4]_s$ laminated plate at multiple locations. The dimensions of the plate were 200 × 200 × 2 mm. The material properties for each unidirectional lamina were

$$E_1 = 121.6 \text{ GPa} \qquad E_2 = 9.17 \text{ GPa}$$
$$G_{12} = 5.27 \text{ GPa} \qquad \nu_{12} = 0.29 \tag{29}$$
$$\rho = 1553 \text{ kg/m}^3$$

Each of the impact locations in a multiple impact event was generated randomly using a random number generator. On the other hand, the corresponding impact force was constructed as

$$P_i(t) = \begin{cases} 1000 \sin\left(\dfrac{\pi t}{T}\right) + \displaystyle\sum_{j=2}^{10} 100 C_{ij} \sin\left(\dfrac{j\pi t}{T}\right) \\ \qquad i = 1, \ldots, L, 0 \leq t \leq T \\ 0 \qquad t > T \end{cases} \tag{30}$$

The value C_{ij} was generated randomly, and L is the number of impact forces exerted at the plate. The summation terms for $j = 2, \ldots, 10$, were further adjusted such that the impact force $P_i(t) > 0$, i.e., $P_i(t)$ in compression. The period T was 400 μs. The total recording time was 700 μs. The highest frequency content of the impact force in Eq. (30) was 12.5 kHz. Thus, 10 beam functions in both the x and y directions were employed, whose highest mode was on the order of 20 kHz. The time step selected was 2 μs. Therefore, a total of 350 time steps was needed for every impact event.

A typical example for impact at multiple locations on the laminate is shown in Figs. 2–5, in which two impact forces acted simultaneously, and strains at four locations were used as the input data for force identification purposes. The coordinates of the two impact locations were (100, 61) and (59, 106) mm; and the four strain locations were (55, 50), (150, 55), (145, 150) and (50, 145) mm, as illustrated in Fig. 2. It has been found that use of multiple gauges, which results in an overdetermined condition in Eq. (28), gives a better correlation between the identified and the given impact force.[18,21] Thus, in this section, the amount of strain data was always greater than that of the impact forces. This effect of using more input data than required will also be justified experimentally in the next section. The "true" impact forces and the strains are shown in Figs. 3 and 4, in which the "true" strains were obtained by forward calculation using both Eq. (27) and the "true" impact forces as the input data. The identified impact forces are also illustrated in Fig. 3. The agreement is very satisfactory. The slight deviation between the identified and the true force histories at close to the end of the impact event was due to the characteristics of the convolution integral. On the other hand, the identified and the true strains shown in Fig. 4 coincide exactly.

In an optimization problem, the convergent criterion is always critical for the quality of the obtained solution. To obtain the optimal convergent criterion for the problem, the value of the error function in Eq. (28) and the corresponding convergent rate $|\Delta E/E|$ are plotted in Fig. 5. It has been shown that the convergent criterion

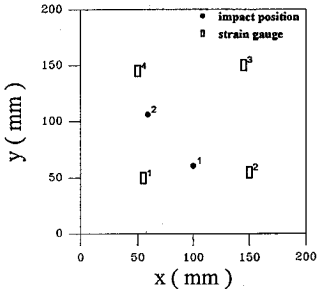

Fig. 2 Positions for the calculated strains and the impact forces.

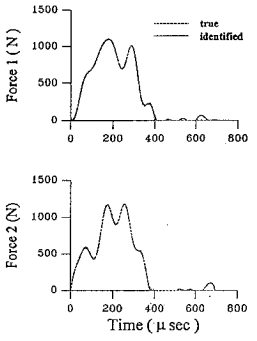

Fig. 3 True and identified impact forces.

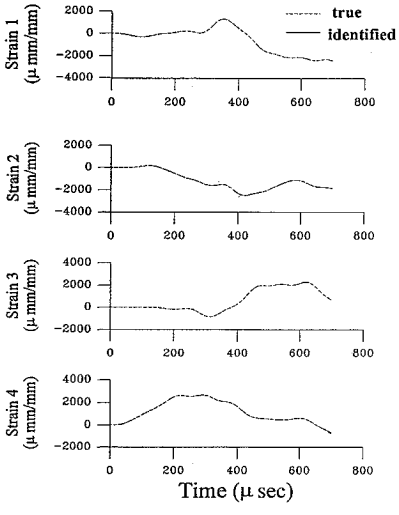

Fig. 4 True and identified strain histories.

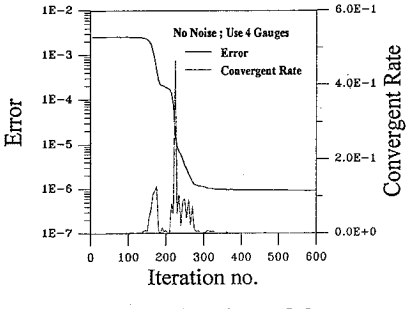

Fig. 5 Values of the error function and the convergent rate.

can be set at an iteration number after which the value of the error function becomes not much changed.[21,23] This method of selecting the convergent criterion is adopted in this study. Thus, in this example, an iteration number of 500 was used as the convergent criterion.

Effect of Noise

Because signals recorded in an impact event are always contaminated with noise to a certain extent, the method developed in the previous section is to verify for applicability under such conditions. In this subsection, randomly generated noise, which is considered to be uncorrelated, is added to the "true" signals previously shown in Fig. 4. In the next section, impact responses recorded from experiment, which are contaminated with both correlated and uncorrelated noise, are further used to verify the developed method. The signal-to-noise ratio is defined as

$$S/N \text{ ratio} = \frac{S_{\max} - S_{\min}}{N_{\max} - N_{\min}} \tag{31}$$

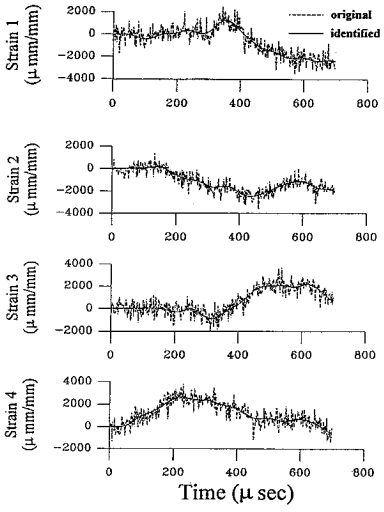

Fig. 6 Original noisy strains and identified strains at the four locations shown in Fig. 2.

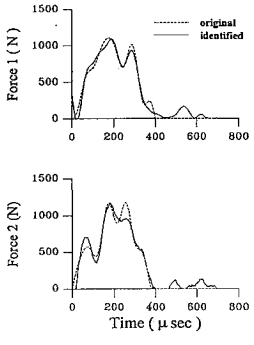

Fig. 7 Original impact forces and those identified using the noisy strains in Fig. 6.

where $S_{\max}$ and $S_{\min}$ represent the values of the maximum and the minimum signals in an impact event, and $N_{\max}$ and $N_{\min}$ are the noise of the maximum and the minimum values, respectively. In this study, the S/N ratio is set to be 1.0; i.e., the maximum difference in amplitude for the signals and for the noise are of the same magnitude. This noise was generated using a random number generator and was in the Gaussian distribution with zero mean and with the standard deviation of 1.0. These noise-contaminated strains, called the "original" strains in this study, are shown in a typical example as the broken curves in Fig. 6, in which noise of the S/N ratio of 1.0 was added to the true strains in Fig. 4. On the other hand, the "original" impact forces shown as the broken curves in Fig. 7 are identical to those of the true forces in Fig. 3. Also shown in Fig. 7 are the identified impact forces, which used the four noisy original strains in Fig. 6 as the input data. The agreement between the original and the identified forces is considered to be satisfactory. The identified strains, which were forward calculated directly using Eq. (27) and using the identified forces in Fig. 7 as the input data, are also illustrated in Fig. 6. It was found that the effect of the added noise was suppressed and that the identified strains generally passed through the mean of the noise carried on the true strains.

Experimental Verification

Setup and Procedure

The experimental setup for verification of the developed method is shown in Fig. 8. A free-supported T300/976 Gr/ep laminated plate of $[0_4^\circ/90_4^\circ]_s$ stacking sequence was used. The material properties are listed in Eq. (29). The dimensions of the plate were 142 × 141.2 × 2 mm. Three KYOWA KFG-2-350-C1-11 strain gauges were mounted on the impact side of the plate at locations no. 1: $\epsilon_{yy}(41.0, 40.6)$, no. 2: $\epsilon_{yy}(91.0, 70.6)$, and no. 3: $\epsilon_{yy}(41.0, 100.6)$. The strains were properly amplified using KYOWA CDV230C signal conditioners, whose cutoff frequency

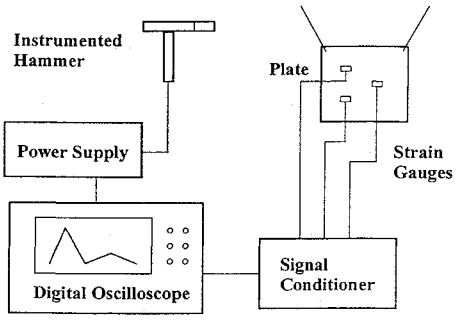

Fig. 8 Schematic for the experimental setup.

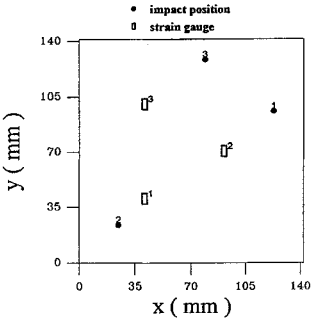

Fig. 9 Locations of impact and strain gauges.

was 200 kHz. On the other hand, impact was conducted using a PCB 086B01 SN6445 instrumented hammer. A four-channel Nicolet oscilloscope was used to record the impact-induced strains and forces. Because of the number-of-channel limitation, the multiple-impact condition was simulated by adding the strain data from several single-impact events. This is considered to be applicable because each impact force exerted by the instrumented hammer was small, and the plate was in the elastic state with very small strain values. Thus, the superposition principle is considered to be applicable.

To help identify the impact locations, the hammer head was marked with chalk. This hammer head was 3 mm in diameter. Thus, the exerted impact force could be treated as a point load. All of the recorded signals, including the impact forces and the strains, were directly transmitted to a PC through an IEEE-488 interface card without any filtering process. In all of the impact tests, the sampling rate used in the oscilloscope was 1 μs.

Results and Discussion

Figure 9 shows a typical example, in which three impact forces acted on the same laminated plate at the same time. The impact locations were (123.0, 96.0), (24.5, 24.0), and (79.0, 128.5) mm. The strain histories corresponding to this impact event are illustrated in Fig. 10. Also shown in this figure are the identified strains, which will be discussed later.

To decide how many vibration modes are needed in the analysis, the frequency spectrum of the recorded strains needs to be obtained. Figure 11 illustrates a typical energy spectrum, which was obtained through fast Fourier transform using the signals in gauge 1 in Fig. 10. The energy contents of this strain were found to be mostly within 60 kHz. Thus, 14 × 14 beam functions were used to construct the displacement field in Eq. (2). The natural frequency corresponding to the highest mode was 70.6 kHz.

The measured impact forces in this triple-impact test and the corresponding identified forces are shown in Fig. 12, in which the latter forces were obtained using the measured strains in Fig. 10 as the input data. The time step used in this example and in the subsequent analyses was always $\Delta t = 4\ \mu$s. The overall agreement is considered to be reasonable. The rise time, the force peaks, and the phases for all three identified impact forces are in good agreement with the measured values. The deviation may be due to the effects of noise, the experimental limitation, and the difference between

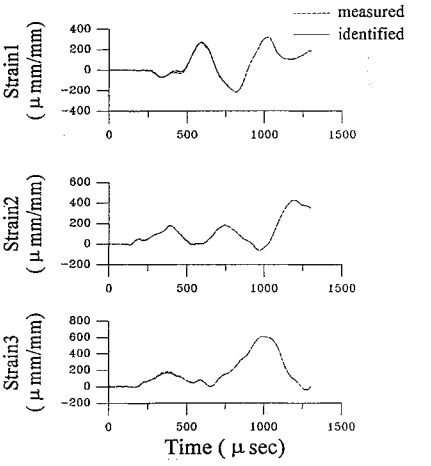

Fig. 10 Measured and identified strain histories.

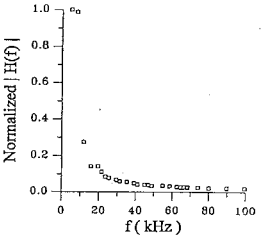

Fig. 11 Frequency spectrum of the strains recorded at gauge —in Fig. 10.

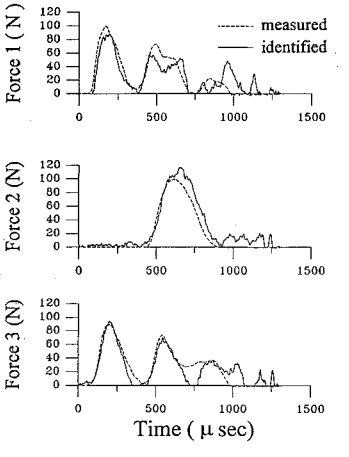

Fig. 12 Measured and identified impact forces.

the actual laminated plate and the mathematical model constructed using the classical laminate theory and the Rayleigh-Ritz method.

Another cause of the deviation was that the number of the unknowns $\boldsymbol{P}_i, i = 1, 2, 3$, was identical to the number of the strain data. Thus, this is a determined situation in an optimization problem. It has been found that this is the worst situation for obtaining an optimal impact force history.[18,21,23] In the examples illustrated later, better correlation is always obtained if the number of input strain data is greater than that of the unknown forces.

Also shown in Fig. 10 are the identified strains. These strains were directly calculated using Eq. (27) and by using the identified impact force histories in Fig. 12. The correlation between the measured and the identified strains is much better than that of the impact forces.

Impact Location Identification

Impact location identification is a very difficult task. When the rise time of an arrival signal is short, the arrival time method has been used along with the wave theory.[24] Unfortunately, this approach is not applicable to low-velocity-impact problems because the arrival time of the signals is difficult to identify.[23] A new method was

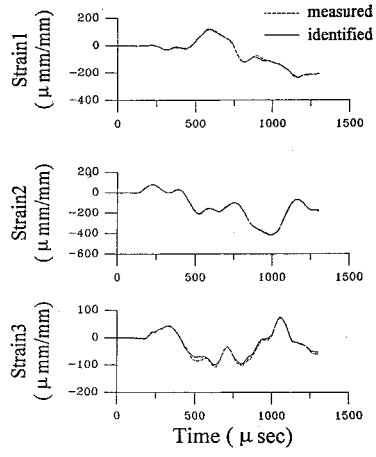

Fig. 13 Measured and identified strain histories.

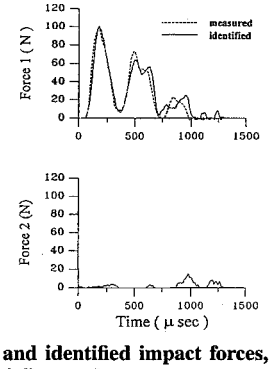

Fig. 14 Measured and identified impact forces, the force exerted at location 2 was essentially equal to zero.

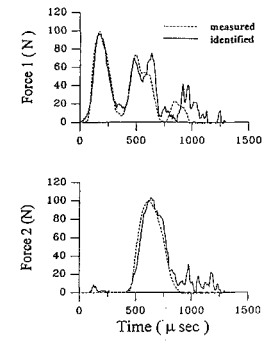

Fig. 15 Measured and identified forces obtained from incomplete strains.

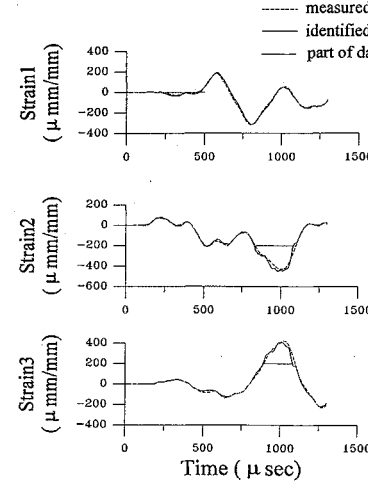

Fig. 16 Measured incomplete strains and reconstructed strains.

recently developed to identify the location of impact when a plate was subjected to single strike at low velocities.[25,26] In this section, the method developed in this paper is further applied to search for the actual impact points among several candidate locations on a composite laminate. Because of the limitation of the channel number for the oscilloscope used and also to preserve the overdetermined situation, two suspected impact locations are selected, but only one of the locations is the actual impact point. The recorded strains are shown in Fig. 13 as the broken curves, and the impact force was exerted at either location 1 or location 2 in Fig. 9. To identify the actual impact location, the impact forces were assumed to apply at both locations. The method developed in a previous section was then employed to solve the problem. The identified impact forces are illustrated in Fig. 14 as the solid curves. From this figure it was found that the laminate was struck at location 1 and that the "force" obtained at location 2 was essentially the noise.

In Fig. 14, the measured impact force is also plotted and is identical to force 1 in Fig. 12. It is clearly found that the identified force in this example is in better agreement with the measured force than is that shown as force 1 in Fig. 12, which corresponds to a determined situation. This is because the total number of strain data shown in Fig. 13 is 1.5 times more than that of the "two" unknown force histories in Fig. 14. This was thus an overdetermined problem during the search process of the impact forces. Therefore, in a single- or multiple-impact event, once the actual impact locations, whose total number is $L = m_1$, are identified among the candidate locations of $L = m_2$, $m_2 > m_1$, the analysis using the developed method can always be performed once more by using Eq. (28) with $L = m_1$ instead of $L = m_2$ to search for the impact force histories. In such a situation, because the data ratio between the responses and the unknown forces increases, a better correlation between the identified and the measured forces can always be achieved.

Reconstruction of Incomplete Strains

In an impact event, sometimes a portion of the recorded structural responses is missing. This situation usually happens when an improper triggering level is set to record the transient signals or when the magnitudes of the signals are unexpectedly large at certain time intervals during impact, resulting in an overflow problem. In the former situation, the data at the beginning of an impact event are missing, whereas, in the latter situation, the data may be lost anytime during impact. If either of these situations occurs, one usually needs to redo the experiment. As a result, there needs extra cost and additional time is consumed. In this section, the previously developed method is applied with a minor modification to reconstruct the lost data.

As a typical example, the measured impact forces are shown as the broken curves in Fig. 15. These forces were exerted at locations 1 and 2 in Fig. 9. The recording period was 1400 μs. However, as shown in Fig. 16, the following strains were missing: 1) gauge 1: 0–500 μs, 2) gauge 2: 836–1096 μs, and 3) gauge 3: 896–1096 μs. Thus, the numbers of the lost data were 125, 60, and 50, respectively, because $\Delta t = 4$ μs. Therefore, for gauge 1, Eq. (25) is changed to

$$\begin{Bmatrix} r_p \\ r_{p+1} \\ \vdots \\ r_n \end{Bmatrix} = \sum_{i=1}^{L} \begin{bmatrix} G_p & G_{p1} & \cdots & G_1 & & \\ G_{p+1} & G_p & \cdots & \cdots & G_1 & \\ \vdots & \vdots & \vdots & \vdots & \vdots & \ddots \\ G_n & G_{n-1} & G_{n-2} & \cdots & \cdots & \cdots & G_1 \end{bmatrix}_i \begin{Bmatrix} P_1 \\ P_2 \\ P_3 \\ \vdots \\ P_n \end{Bmatrix}_i \tag{32}$$

where $p = 125$, $n = 350$ and $L = 3$. Similarly, the general expression for gauges 2 and 3 is

$$\begin{Bmatrix} r_1 \\ \vdots \\ r_p \\ r_q \\ \vdots \\ r_n \end{Bmatrix} = \sum_{i=1}^{L} \begin{bmatrix} G_1 & & & & & & & \\ \vdots & \ddots & & & & & & \\ G_p & \cdots & G_1 & & & & & \\ G_q & G_{q-1} & \cdots & \cdots & \cdots & G_1 & & \\ \vdots & \vdots & \vdots & \vdots & \vdots & \cdots & \ddots & \\ G_n & G_{n-1} & G_{n-2} & \cdots & \cdots & \cdots & \cdots & G_1 \end{bmatrix}_i \times \begin{Bmatrix} P_1 \\ P_2 \\ P_3 \\ \vdots \\ P_n \end{Bmatrix}_i \tag{33}$$

where p and q are 209 and 274 for gauge 2 and 224 and 274 for gauge 3, respectively. Thus, by substituting Eqs. (32) and (33) into Eq. (28), one can obtain the optimal impact force histories accordingly. The identified impact forces are shown as the solid curves in Fig. 15. Once the impact forces were identified, the lost strain data were reconstructed using Eq. (27). These results are shown in Fig. 16, in which the reconstructed strains are in very good agreement with the measured strains.

The only limitation for the reconstruction of the lost strains is that the number of unknown force data must be smaller than that of the strains that have not been lost. Thus, within this limitation any portions of the strains that are lost in an impact event can be reconstructed. In this example, the number of strain data was $3 \times 350 - 125 - 65 - 50 = 810$. On the other hand, the number of unknowns is $700 < 810$. Thus, this was within the limitation. Further, because this is in an overdetermined situation, the identified impact forces are in better agreement with the measured forces than are those in Fig. 12, which is in the determined situation.

Conclusions

The analytical method for identification of impact force histories exerted at multiple locations on a laminated composite plate has been presented. This method begins with construction of approximate Green's functions by using the classical lamination theory, the Rayleigh-Ritz method, and the modal superposition method. The gradient projection method has been successfully adopted to search for the optimal impact force histories. This method has been verified using both randomly generated numerical signals with a signal-to-noise ratio of 1.0 and experimental data. The agreement in all of the comparisons was satisfactory. This method was then applied to identify the actual impact points among several candidate locations at which the plate was possibly hit. The method was further applied with slight modification to reconstruct the incomplete strain data in an impact event. This situation is frequently encountered in an impact event. It has also been found that the use of signals from more gauges than required always helps identify the impact force histories with better accuracy.

Acknowledgment

This work was supported by the National Science Council of Taiwan, Republic of China, under Contract NSC 82-0405-E-002-086.

References

[1]Tan, T. M., and Sun, C. T., "Use of Statical Indentation Laws in the Impact Analysis of Laminated Composite Plates," *ASME Journal of Applied Mechanics*, Vol. 52, 1985, pp. 6–12.

[2]Wu, E., and Shyu, K., "Response of Composite Laminates to Contact Loads and Relationship to Low-Velocity Impact," *Journal of Composite Materials*, Vol. 27, No. 15, 1993, pp. 1443–1464.

[3]Hertz, H., "Uber die Beruhrung fester Elastischer Korper," *Journal for die reine und angewandte mathematik*, Vol. 92, 1881, pp. 156–171., translated by D. E. Jones and G. A. Schott, MacMillan and Co., London, England, UK, 1896.

[4]Wu, E., and Yen, C. S., "The Contact Behavior Between Laminated Composite Plates and Rigid Spheres," *ASME Journal of Applied Mechanics*, Vol. 61, 1994, pp. 60–66.

[5]Cairns, D. S., and Lagace, P. A., "Thick Composite Plates Subjected to Lateral Loading," *ASME Journal of Applied Mechanics*, Vol. 54, 1987, pp. 611–615.

[6]Sun, C. T., and Chen, J. K., "On the Impact of Initially Stressed Composite Laminates," *Journal of Composite Materials*, Vol. 19, Nov. 1985, pp. 490–504.

[7]Chen, J. K., and Sun, C. T., "Dynamic Large Deflection Response of Composite Laminates Subjected to Impact," *Composite Structures*, Vol. 4, 1985, pp. 59–73.

[8]Choi, H. Y., and Chang, F. K., "A Model for Predicting Damage in Graphite/Epoxy Laminated Composites Resulting from Low-Velocity Point Impact," *Journal of Composite Materials*, Vol. 26, No. 14, 1992, pp. 2134–2169.

[9]Jang, B. P., Huang, C. T., Hsieh, C. Y., Kowbel, W., and Jang, B. Z., "Repeated Impact Failure of Continuous Fiber Reinforced Thermoplastic and Thermoset Composites," *Journal of Composite Materials*, Vol. 25, Sept. 1991, pp. 1171–1203.

[10]Lee, S.-W. R., and Sun, C. T., "A Quasi-Static Penetration Model for Composite Laminates," *Journal of Composite Materials*, Vol. 27, No. 3, 1993, pp. 251–271.

[11]Zhu, G., Goldsmith, W., and Dharan, C. K. H., "Penetration of Laminated Kevlar by Projectiles—I. Experimental Investigation and II. Analytical Model," *International Journal of Solids and Structures*, Vol. 29, 1992, pp. 399–436.

[12]Wu, E., Tsai, C. Z., and Chen, Y. C., "Penetration into Glass/Epoxy Composite Laminates," *Journal of Composite Materials* (to be published).

[13]Michaels, J. E., and Pao, Y.-H., "Determination of Dynamic Forces from Wave Motion Measurements," *ASME Journal of Applied Mechanics*, Vol. 53, 1986, pp. 6–12.

[14]Chang, C., and Sachse, W., "Analysis of Elastic Wave Signals from an Extended Source in a Plate," *Journal of the Acoustical Society of America*, Vol. 77, 1985, pp. 1335–1341.

[15]Doyle, J. F., "Further Developments in Determining the Dynamic Contact Law," *Experimental Mechanics*, Vol. 24, No. 4, 1984, pp. 265–270.

[16]Doyle, J. F., "Experimentally Determining the Contact Force During the Transverse Imapct of an Orthotropic Plate," *Journal of Sound and Vibration*, Vol. 118, No. 3, 1987, pp. 441–448.

[17]Hollandsworth, P. E., and Busby, H. R. "Impact Force Identification Using the General Inverse Techndique," *International Journal of Imapct Engineering*, Vol. 8, 1989, pp. 315–322.

[18]Wu, E., Tsai, T. D., and Yen, C. S., "Two Methods for Determining Impact Force History on Elastic Plates," *Experimental Mechanics* (to be published).

[19]Cairns, D. S., and Lagace, P. A., "Transient Response of Graphite/Epoxy and Kevlar/Epoxy Laminates Subjected to Imapct," *AIAA Journal*, Vol. 27, No. 11, 1989, pp. 1590–1596.

[20]Qian, Y., and Swanson, S. R., "A Comparison of Solution Techniques for Impact Response of Composite Plates," *Composite Structures*, Vol. 14, 1990, pp. 177–192.

[21]Wu, E., Yeh, J. C., and Yen, C. S., "Impact on Composite Laminated Plate: An Inverse Method," *International Journal of Impact Engineering*, Vol. 15, No. 4, 1994, pp. 417–433.

[22]Haug, E. J., and Arora, J. S., *Applied Optimal Design*, Wiley, New York, 1979.

[23]Yeh, J. C., "Detection of Single, Multiple and Moving Impact Forces on Rectangular Laminated Plates," M.S. Thesis, National Taiwan Univ. Taipei, Taiwan, Republic of China, 1993 (in Chinese).

[24]Pao, Y. H., "Theory of Acoustic Emission," *Elastic Waves and Nondestructive Testing of Materials*, ASME AMD Vol. 29, 1978, pp. 107–128.

[25]Yen, C. S., and Wu, E., "On the Inverse Problem of Rectangular Plates Subjected to Elastic Impact, Part 1: Method Development and Numerical Verification," *ASME Journal of Applied Mechanics* (to be published).

[26]Yen, C. S., and Wu, E., "On the Inverse Problem of Rectangular Plates Subjected to Elastic, Part 2: Experimental Verification and Further Applications," *ASME Journal of Applied Mechanics* (to be published).